MOLECULAR AND CELLULAR BIOLOGY, May 2006, p. 3728–3737 Vol. 26, No. 10
0270-7306/06/$08.00+0 doi:10.1128/MCB.26.10.3728–3737.2006

Nickel Ions Increase Histone H3 Lysine 9 Dimethylation and Induce Transgene Silencing

Haobin Chen, Qingdong Ke, Thomas Kluz, Yan Yan,† and Max Costa*

Nelson Institute of Environmental Medicine, New York University Medical Center, 57 Old Forge Road, Tuxedo, New York 10987

Received 28 December 2005/Returned for modification 6 February 2006/Accepted 6 March 2006

We have previously reported that carcinogenic nickel compounds decreased global histone H4 acetylation and silenced the *gpt* transgene in G12 Chinese hamster cells. However, the nature of this silencing is still not clear. Here, we report that nickel ion exposure increases global H3K9 mono- and dimethylation, both of which are critical marks for DNA methylation and long-term gene silencing. In contrast to the up-regulation of global H3K9 dimethylation, nickel ions decreased the expression and activity of histone H3K9 specific methyltransferase G9a. Further investigation demonstrated that nickel ions interfered with the removal of histone methylation in vivo and directly decreased the activity of a Fe(II)–2-oxoglutarate-dependent histone H3K9 demethylase in nuclear extract in vitro. These results are the first to show a histone H3K9 demethylase activity dependent on both iron and 2-oxoglutarate. Exposure to nickel ions also increased H3K9 dimethylation at the *gpt* locus in G12 cells and repressed the expression of the *gpt* transgene. An extended nickel ion exposure led to increased frequency of the *gpt* transgene silencing, which was readily reversed by treatment with DNA-demethylating agent 5-aza-2′-deoxycytidine. Collectively, our data strongly indicate that nickel ions induce transgene silencing by increasing histone H3K9 dimethylation, and this effect is mediated by the inhibition of H3K9 demethylation.

Posttranslational modifications of histone N-terminal tails are important in chromatin organization, gene transcription, and DNA replication and repair (19). To date, a diverse array of histone modifications has been identified, including acetylation, methylation, phosphorylation, and ubiquitination (28). Among them, methylation of histone H3 lysine 9 (H3K9) is one of the best-studied modifications. H3K9 may be mono-, di-, or trimethylated without changing the positive charge of the lysine residue. Trimethylated H3K9 is typically connected with constitutive heterochromatin, while mono- and dimethylated H3K9 are mainly located in euchromatin and generally linked to repressed promoter regions (29). Suv39h family enzymes are responsible for trimethylation of H3K9 in vivo (27, 29), while G9a and GLP/EuHMTase 1 are two major histone methyltransferases responsible for H3K9 dimethylation in vivo (35, 36). Genetic ablation of either G9a or GLP/EuHMTase 1 dramatically diminished global H3K9 dimethylation in mouse embryonic stem cells (35, 36).

Methylation of histone lysines had long been thought of as a "permanent" modification since there was no known enzyme to demethylate. However, this dogma was challenged by the recent discoveries of histone H3 lysine 4 (H3K4) demethylase LSD1 and H3 lysine 36 (H3K36) demethylase JHDM1 (JmjC domain-containing histone demethylase 1) (32, 39). Although both LSD1 and JHDM1 can remove the methyl group from lysine residues on histone H3, they utilize different mechanisms to demethylate. LSD1 is a flavin-dependent amine oxidase and removes the methyl group from mono- or dimethyl H3K4 by catalyzing the oxidation of amine to an imine intermediate (32). The imine intermediate is then hydrolyzed to form an unstable carbinolamine, which releases one formaldehyde molecule and thus completes the removal of one methyl group (32). Differently from LSD1, JHDM1 belongs to an iron- and 2-oxoglutarate-dependent dioxygenase family, and its JmjC domain is critical for the binding of both Fe(II) and 2-oxoglutarate (39). Similar to the removal of methylation from 1-methyladenine and 3-methylcytosine catalyzed by DNA repair enzyme AlkB (13, 37), JHDM1 demethylates H3K36 by catalyzing the generation of highly reactive oxygen species to attack the methyl group in substrates (39). The oxidized product is unstable and spontaneously releases one formaldehyde molecule, which results in the removal of one methyl group from H3K36 (39). To date, more than 100 JmjC domain-containing proteins have been identified (1, 7). Although LSD1 has been reported to demethylate H3K9 dimethylation when associated with the androgen receptor (24), it is still likely that one of these JmjC domain-containing proteins is responsible for the oxidative demethylation on H3K9 as proposed by Trewick et al. (38).

Nickel compounds are highly carcinogenic but exhibit insignificant mutagenic activity (21). By using Chinese hamster V79-derived cell clones that possess a single copy of the *gpt* (bacterial xanthine guanine phosphoribosyltransferase) transgene inserted either near the telomere of chromosome 1 (G12 cells) or into euchromatin on chromosome 6 (G10 cells), we were able to demonstrate that water-insoluble nickel compounds (NiS and Ni_3S_2) silenced the transgene via epigenetic mechanisms in G12 cells but not in G10 cells (21). It is helpful to know that the loss of endogenous *hprt* (hypoxanthine guanine phosphoribosyltransferase) function in G12 cells makes it possible to select the activation or inactivation of the transgene

* Corresponding author. Mailing address: Nelson Institute of Environmental Medicine, New York University School of Medicine, 57 Old Forge Road, Tuxedo, NY 10987. Phone: (845) 731-3515. Fax: (845) 351-2118. E-mail: costam01@nyu.edu.

† Present address: Faculty of Life Science, Northwestern Polytechnical University, 127 Youyi West Road, Xi'an, Shaanxi 710072, People's Republic of China.

gpt by resistance to hypoxanthine-aminopterin-thymidine (HAT) or 6-thioguanine (6-TG), respectively. In support of the epigenetic nature of the transgene silencing, the *gpt* promoter in Ni-induced 6-TG-resistant (6-TG^r) variants was found to associate with a decrease in histone H3 and H4 acetylation, as well as an increase in histone H3K9 dimethylation, DNA methylation, and chromatin condensation (22, 40). Furthermore, the *gpt* gene function can be restored following treatment with histone deactylase trichostatin A or DNA-demethylating agent 5-azacytidine (22, 34). Interestingly, insoluble nickel compounds were found to decrease the global level of histone H4 acetylation in both yeast and mammalian cells (3). Recently, two independent groups reported that exposure to nickel ions also decreased global histone acetylation in mammalian cells (15, 20).

Although it is clear that nickel compounds silence genes through epigenetic mechanisms, it is still unknown how the epigenetic changes are initiated and dynamically involved in gene silencing. Here we reported that nickel ions increased global H3K9 dimethylation in several mammalian cell lines. We attribute this increase of H3K9 dimethylation to the Ni(II)-induced inhibition of the demethylation process. To our knowledge, we are the first to demonstrate the H3K9 demethylation activity that is catalyzed by an as-yet-unidentified Fe(II)–2-oxoglutarate-dependent histone demethylase(s). The presence of nickel ions substantially decreased the activity of this unidentified histone demethylase. In addition, extended exposure of G12 cells to low concentrations of nickel ions can directly increase the H3K9 dimethylation at the promoter region of the *gpt* transgene, which likely leads to DNA methylation and the silencing of the gene. These results suggest that the inhibition of the histone demethylation process and the subsequent increase of H3K9 dimethylation may play a pivotal role in nickel-induced gene silencing and carcinogenesis.

MATERIALS AND METHODS

Cell culture. Human lung carcinoma A549 cells were grown in Ham's F-12–K medium (Gibco, Grand Island, NY), supplemented with 10% fetal bovine serum (FBS; Omega Scientific, Inc., Tarzana, CA). Human embryonic kidney 293 (HEK 293) and mouse embryo fibroblast Pw cells were grown in Dulbecco modified Eagle medium (DMEM) (Gibco) supplemented with 10% FBS. Human osteosarcoma cells were grown in α minimal essential medium (Gibco) supplemented with 10% FBS. Mouse embryonic stem cells were maintained in DMEM supplemented with 10% FBS and 1×10^3 units/ml murine ESGRO (Chemicon, Temecula, CA). The transgenic *gpt*$^+$ *hprt*$^-$ G12 cells were cultured in F-12 medium (Gibco) supplemented with 5% FBS. To maintain a low spontaneous mutation frequency, G12 cultures were supplemented with HAT. One day prior to treatment, the cells were removed from HAT selection. All cells were maintained at 37°C in a humid 5% CO_2 atmosphere.

Chemicals and expression vectors. Dimethyloxalylglycine (DMOG) was purchased from Frontier Scientific (Logan, UT). All other reagents were obtained from Sigma (St. Louis, MO) unless otherwise specified. The green fluorescent protein (GFP)-tagged human G9a expression vector, EGFP-hG9a, and its set domain deletion mutant expression vector, EGFP-hG9a ΔSET, were kindly provided by M. Walsh (25).

Preparation of nuclear extracts and histones. The nuclear extract was prepared using a CelLytic NuCLEAR extraction kit (Sigma). To extract histones, the monolayer cells were lysed in ice-cold radioimmunoprecipitation assay (RIPA) buffer (Santa Cruz Biotechnology, Santa Cruz, CA) supplemented with a protease inhibitor mixture (Roche Applied Sciences, Indianapolis, IN) for 10 min. The sample was then collected and centrifuged at 10,000 × *g* for 10 min. The pellet was washed once in buffer W (10 mM Tris-Cl, pH 7.4, and 13 mM EDTA), and resuspended in 200 μl 0.4 N H_2SO_4. After incubation on ice for 90 min, the sample was centrifuged at 14,000 × *g* for 15 min. The supernatant was mixed with 1 ml cold acetone and kept at −20°C overnight. The histones were collected by centrifugation at 14,000 × *g* for 15 min. After one wash with acetone, the histones were air dried and resuspended in 4 M urea.

Western blot assays. Equal amounts of histones (5 μg) were separated in a 15% SDS-polyacrylamide gel and then transferred to a polyvinylidene difluoride (PVDF) membrane. Immunoblotting was performed with 1:2,000-diluted dimethyl H3K9 (Upstate Biotechnology Inc., Lake Placid, NY), 1:1,000-diluted monomethyl H3K9 (Upstate), or 1:400-diluted trimethyl H3K9 (Abcam, Cambridge, MA) antibodies. The primary antibody was detected by chemical fluorescence following an ECL Western blotting protocol (Amersham, Piscataway, NJ). After transfer to a PVDF membrane, the gel was stained with Bio-safe Coomassie blue stain (Bio-Rad, Hercules, CA) to assess the loading of histones.

To detect G9a and Suv39h1 in whole-cell extract, approximately 5×10^6 cells in each 10-cm dish were lysed with 250 μl boiling lysis buffer (1% SDS, 1.0 mM sodium orthovanadate, and 10 mM Tris, pH 7.4). The scraped cells were transferred to an Eppendorf tube and boiled for 5 min. To reduce viscosity, the samples were sonicated by applying 10 1-s pulses with a Branson Sonifier 450 (Branson Ultrasonics Co., Danbury, CT). After the samples were centrifuged at 14,000 × *g* for 5 min, the supernatant was collected for Western blotting. The supernatant containing 200 μg protein was separated in an SDS-polyacrylamide gel and transferred to a PVDF membrane. Immunoblotting was performed with 1:500-diluted G9a (Upstate) or Suv39h1 (Upstate) antibodies. To detect G9a in nuclear extract, the nuclear extract containing 40 μg protein was used for Western blotting. To detect overexpressed GFP-hG9a or GFP-hG9a ΔSET fusion protein in whole-cell RIPA lysate, the lysate containing 75 μg protein was separated in a 7.5% SDS-polyacrylamide gel. The immunoblotting was performed with 1:200-diluted GFP antibody (Santa Cruz Biotechnology).

After immunoblotting, the membrane was incubated with the stripping buffer (50 mM glycine, pH 10.8, 7 M guanidine hydrochloride, 50 μM EDTA, 100 mM KCl, and 20 mM 2-mercaptoethanol) for 6 min. The membrane was then washed with H_2O three times for 15 min per wash and reprobed with α-tubulin (Sigma) or c-*myc* (Santa Cruz Biotechnology) antibodies to assess the protein loading. The immunoblots were scanned and subjected to densitometric analysis by Kodak 1D 3.52 for Macintosh, and values were normalized to that obtained in the control sample(s).

Transient transfection. Transient transfection was performed in HEK 293 cells using Lipofectamine 2000 (Invitrogen, Carlsbad, CA) following the manufacturer's protocol. Twenty-four h after transfection, the cells were exposed to 1 mM $NiCl_2$ for an additional 24 h. Cells were lysed in ice-cold RIPA lysis buffer supplemented with a protease inhibitor mixture. After incubation on ice for 10 min, the scraped lysate was centrifuged at 10,000 × *g* for 10 min at 4°C. The supernatant was used either for Western blotting or for the in vitro histone H3K9 methyltransferase (HKMT) assay.

In vitro HKMT activity assay. The supernatant containing 10 mg protein was incubated with anti-GFP antibody (Santa Cruz Biotechnology) on a rotator overnight, and the antibody was immunoprecipitated with protein A/G PLUS agarose (Santa Cruz Biotechnology). The immunoprecipitated complex was immediately used for an in vitro HKMT assay. The immunoprecipitated complex was mixed with 0.8 μg biotin-conjugated histone H3 peptide (amino acids 1 to 21; 2,724 Da; Upstate) and 1.1 μCi *S*-adenosyl-L-[methyl-^{3}H]methionine ([^{3}H]SAM; 13.3 Ci/mmol; Perkin-Elmer, Wellesley, MA) in HMT buffer (50 mM Tris-HCl, pH 9.0, 1 mM phenylmethylsulfonyl fluoride, and 0.5 mM dithiothreitol) in a final volume of 50 μl. After incubation at 30°C for 1 h, 10 μl reaction mixture was spotted onto a P81 phosphocellulose square (Upstate). The P81 square was washed three times with 5 ml ice-cold 0.2 M ammonium bicarbonate solution. The square was then air dried, and its radioactivity was counted with a Wallac Liquid Scintillation Counter model 1409 (Perkin-Elmer). The rest of the reaction mixture was then separated in a 20% SDS-polyacrylamide gel. The gel was treated with En^{3}Hance (Perkin-Elmer), and the radioactivity was visualized by autoradiography.

Histone methylation removal rate measurement. To determine the removal rate of histone methylation, A549 cells were grown in methionine-deficient DMEM (Gibco) supplemented with 0.1 mCi/ml L-[methyl-^{3}H]methionine (Perkin-Elmer) for 24 h. The cells were washed twice with phosphate-buffered saline (PBS) and replenished with F-12–K complete medium supplemented with 1 mM hydroxyurea. After incubation for 24 h, histones were extracted from three samples. Their radioactivity was considered as the amount of ^{3}H labeling on histones following a 24-h chase. Prior to $NiCl_2$ treatment, fresh F-12–K medium supplemented with 1 mM hydroxyurea was replenished. After exposure to 1 mM $NiCl_2$ for an additional 48 h, histones were extracted and the radioactivity was determined as the remaining ^{3}H labeling following a 72-h chase. The radioactivity of histones was measured by a scintillation counter. All treatments were conducted in triplicate.

Histone H3K9 demethylation assay. To prepare the substrate containing ^{3}H-labeled mH3K9, 0.83 μg/50 μl biotin-conjugated histone H3 N-terminal peptide (amino acids 1 to 21; 2,724 Da) was incubated with 1.1 μCi/50 μl [^{3}H]SAM (13.3 Ci/mmol) and 250 ng/50 μl recombinant G9a enzyme (Upstate) in HMT buffer. After overnight incubation at 37°C, the specific activity of ^{3}H-labeled histone substrate was measured by spotting a 1-μl sample onto a P81 phosphocellulose square. For each demethylation reaction, histone substrate with 1×10^4 cpm activity was mixed with 400 μg prewashed streptavidin magnetic particles (Roche Applied Science). After 1 h of incubation at 4°C on a rotator, the magnetic particles were washed three times with buffer A (20 mM K^+-phosphate buffer, pH 7.5, 0.15 mM NaCl). The standard demethylation reaction was performed by incubating 50 μg freshly prepared A549 nuclear extract with [^{3}H]mH3K9 peptide particles in the presence of 50 mM Tris, pH 7.5, 2 μg/ml bovine serum albumin, 0.1 mg/ml catalase, 0.1 mM DL-dithiothreitol, 2 mM ascorbate, 60 μM $FeSO_4$, and 0.5 mM 2-oxoglutarate in a final volume of 50 μl. After overnight incubation at 30°C, the magnetic particles were washed three times with buffer A and resuspended in 200 μl buffer A. Twenty μl suspension was mixed with 5 ml EcoLume (ICN, Costa Mesa, CA), and the radioactivity was measured by a scintillation counter. The experiment was conducted in duplicate.

Northern blot assays. Northern blotting was performed as described previously (40).

Transgene silencing assay. A total of 5×10^5 G12 cells were seeded into 75-cm^2 flasks and exposed to various concentrations of $NiCl_2$ for up to 28 days. The cells were rinsed with PBS twice and incubated in F-12 medium for a 7-day recovery period. Following the recovery period, 2×10^6 cells per sample were reseeded at a maximum cell density of 2×10^5 cells/10-cm dish and grown in F-12 medium containing 10 μg/ml 6-TG for 10 days. The reseeding plating efficiency in nonselective medium (F-12) was also determined. The gene silencing frequency was calculated as the number of colonies growing in the selective medium corrected by the number of clonable cells in nonselective medium.

Reversion assay. The reversion assay was performed as previously described (34). In brief, $NiCl_2$-treated G12 cells that grew in 6-TG selective medium were treated with 4 μM 5-aza-2′-deoxycytidine (5-Aza; Sigma) for 2 days. The cells were then grown in nonselective medium for 1 week, and 2×10^4 cells were seeded into each 10-cm dish and selected with F-12 medium containing HAT. After 2 weeks, HAT-resistant colonies were stained with Giemsa stain.

ChIP assays. Either 1×10^6 or 1×10^7 cells were seeded into a 10- or 15-cm dish, respectively. On the second day, 270 μl 37% formaldehyde per 10 ml growth medium was added into the dishes. After 10 min of incubation at 37°C, the medium was aspirated and the cells were washed with ice-cold PBS twice. After the last wash, the cells were replenished with PBS supplemented with proteinase inhibitor and the cells were collected using a disposable scraper. The cells were spun down at $1{,}000 \times g$ for 5 min, and the pellet was frozen in liquid nitrogen. The chromatin immunoprecipitation (ChIP) assay was performed by following the protocol provided by Upstate. The following set of primers was used for PCR amplification: 5′-TGG CGC GTG AAC TGG GTA T-3′ (sense) and 5′-TGC GAA GAT GGT GAC AAA G-3′ (antisense). To facilitate the detection of PCR product, 0.1 μl [α-^{32}P]dCTP (3,000 Ci/mmol and 10 mCi/ml; Perkin-Elmer) was added into each reaction mixture. The conditions of PCR amplification were 95°C for 2 min and 28 cycles of 95°C for 45 s and 55°C for 45 s, and 72°C for 1 min. The PCR products were then separated in a 5% Tris-buffered EDTA–polyacrylamide gel. The gel was dried, and the radioactivity was visualized by autoradiography.

Statistical analysis. The two-tailed Student *t* test was used to determine the significance of differences between treated sample and control. The difference was considered significant at $P < 0.05$.

RESULTS

Nickel ions increase global H3K9 mono- and dimethylation. To understand the role of H3K9 methylation in Ni-induced gene silencing, we first examined the effects of nickel ions on the global H3K9 methylation in human lung carcinoma A549 cells. Interestingly, nickel ions were found to increase global histone H3K9 mono- and dimethylation but to have no effect on H3K9 trimethylation (Fig. 1a). The Ni(II)-induced H3K9 dimethylation was chosen for further study. As shown in Fig. 1b, global H3K9 dimethylation expression was increased by 250 μM or higher concentrations of Ni ions. Meanwhile, nickel ions also increased H3K9 dimethylation in a time-dependent manner (Fig. 1c). The increase of H3K9 dimethylation began at 12 h, peaked at 24 h, and persisted at later time intervals of nickel ion exposure (Fig. 1c). These results in Fig. 1d demonstrated that an increase of H3K9 dimethylation following nickel ion exposure occurs in cell lines of different lineages.

Nickel ions increase global H3K9 dimethylation by histone methyltransferase G9a-independent mechanisms. It has been known that G9a is one of the primary histone methyltransferases responsible for H3K9 dimethylation in vivo (35). To explore the role of G9a in Ni(II)-induced H3K9 dimethylation, the G9a protein level was examined following nickel ion exposure in A549 cells. In contrast to an increase of H3K9 dimethylation, Ni ions actually decreased G9a expression in A549 cells (Fig. 2a). Interestingly, the expression of Suv39h1, a histone methyltransferase primarily responsible for H3K9 trimethylation, was also decreased following Ni ion exposure (Fig. 2a). A decrease of G9a expression was also observed in the nuclear extract of A549 cells at all three selected time intervals following nickel ion exposure (Fig. 2b).

The change of G9a methyltransferase activity following Ni ion exposure was next examined. Since many other methyltransferases also exhibit H3K9 methyltransferase activity in vitro (35), it was inappropriate to measure G9a methyltransferase activity from a crude nuclear extract. To specifically measure G9a methyltransferase activity, GFP-tagged human G9a (GFP-hG9a) fusion protein was overexpressed in HEK 293 cells and immunoprecipitated for in vitro methyltransferase assay. If the immunoprecipitate possesses G9a activity, it should catalyze the transfer of the ^{3}H-labeled methyl group from [^{3}H]SAM to the H3K9 residue in histone H3 N-terminal peptide. The radioactivity on histone H3 N-terminal peptide was either visualized by autoradiography or measured by a scintillation counter. Since no methyltransferase activity was detected in the samples transfected with G9a deletion mutant vectors, the activity measured in the samples transfected with G9a vectors represented specific G9a activity (Fig. 2c). As shown in Fig. 2c, nickel ion exposure decreased both the expression and activity of overexpressed GFP-hG9a fusion protein. Taken together, these results indicated that nickel ions increased global H3K9 dimethylation through histone methyltransferase G9a-independent mechanisms.

Nickel ions increased H3K9 dimethylation by interfering with demethylation process. To determine the roles of other methyltransferases in Ni(II)-induced H3K9 dimethylation, the cells were incubated in methionine-deficient medium prior to nickel ion exposure. Since methionine is essential for SAM synthesis and SAM has a short half-life in cells (14), the withdrawal of methionine in the culture medium could lead to a lowered intracellular SAM pool and a generalized inhibition of methyl transfer reactions. As shown in Fig. 3a, incubation of cells in methionine-deficient medium dramatically decreased global dimethylated H3K9, indicating that the histone methylation process was impaired by the withdrawal of methionine in the medium. The addition of nickel ions caused no observable toxicity (e.g., cell detachment) in cells under methionine-depleted conditions but still elevated H3K9 dimethylation compared to untreated cells (Fig. 3a). These results indicated that nickel ions likely increased H3K9 dimethylation by inhibiting the demethylation process rather than activating the methylation process.

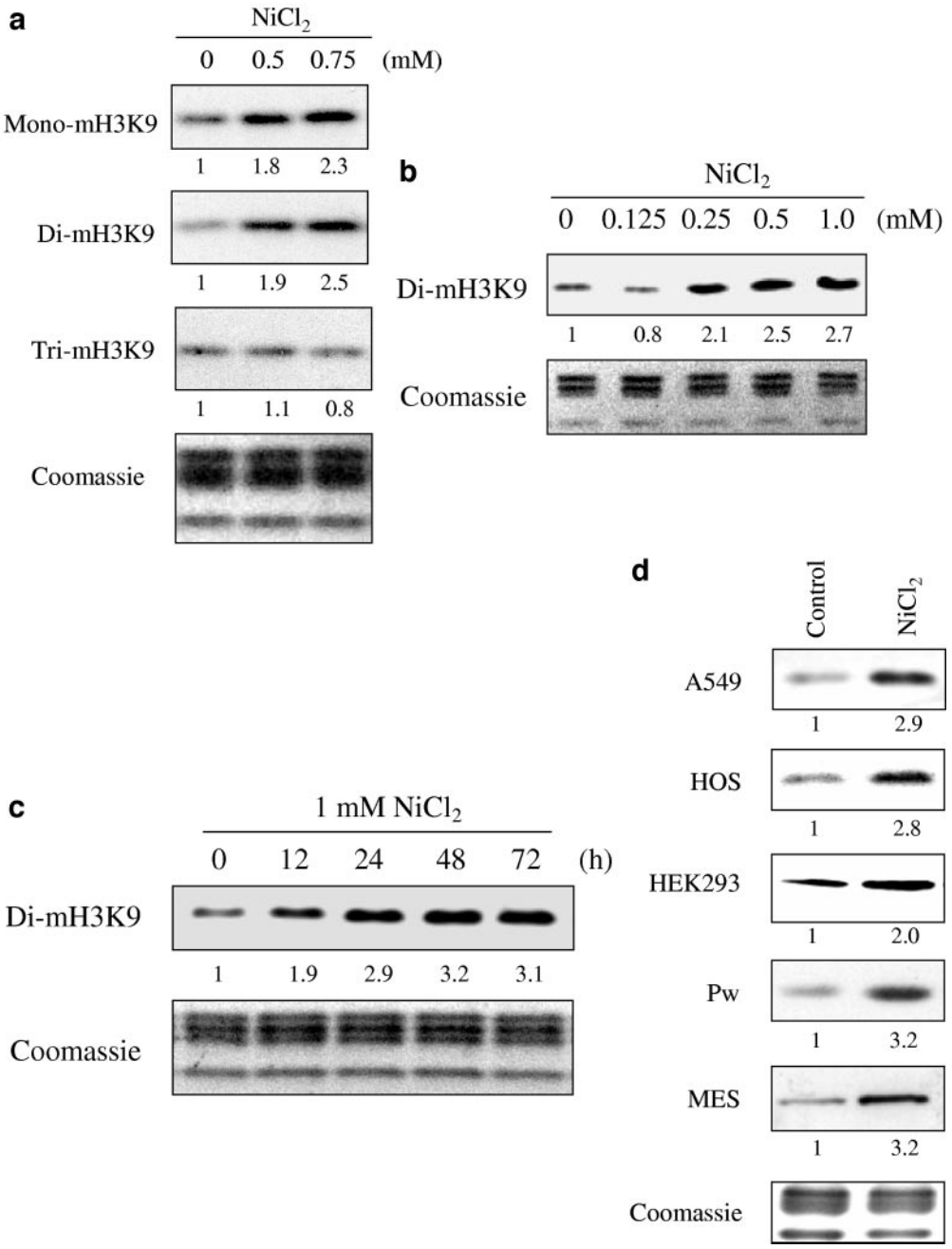

FIG. 1. The changes of global histone H3K9 methylation following nickel ion exposure. (a) A549 cells were exposed to 0.5 mM or 0.75 mM $NiCl_2$ for 24 h. (b) A dose-dependent increase of global H3K9 dimethylation by nickel ions. A549 cells were exposed to various concentrations of $NiCl_2$ for 24 h. (c) A time course study on global H3K9 dimethylation following nickel ion exposure. A549 cells were exposed to 1 mM $NiCl_2$ for selected time intervals as indicated. (d) Exposure to 1 mM $NiCl_2$ for 24 h increased H3K9 dimethylation in different cell types. HOS, human osteosarcoma; MES, murine embryonic stem. Histones were extracted and separated in a 15% SDS-polyacrylamide gel and immunoblotted with various antibodies as indicated. Loading of the histones in all gels was assessed using Coomassie blue staining.

The expression of histone H3K9 methylation is balanced between methylation and demethylation processes. However, the H3K9 demethylation process has not been well understood. Thus, the effects of nickel ions on histone methylation removal were first examined. Intracellular histones and their methylation modifications were labeled with [^{3}H]methionine. To prevent histone synthesis, the cells were then subjected to a 24-h incubation with hydroxyurea, and such a condition has been shown to cause approximately 90% of A549 cells to be arrested in the S phase of the cell cycle (23). In the presence of hydroxyurea, the cells were then subjected to an additional 48-h chase with or without nickel ions in the medium. Without the presence of nickel ions, histone labeling decreased about 50% after an additional 48-h chase (Fig. 3b). Since histone

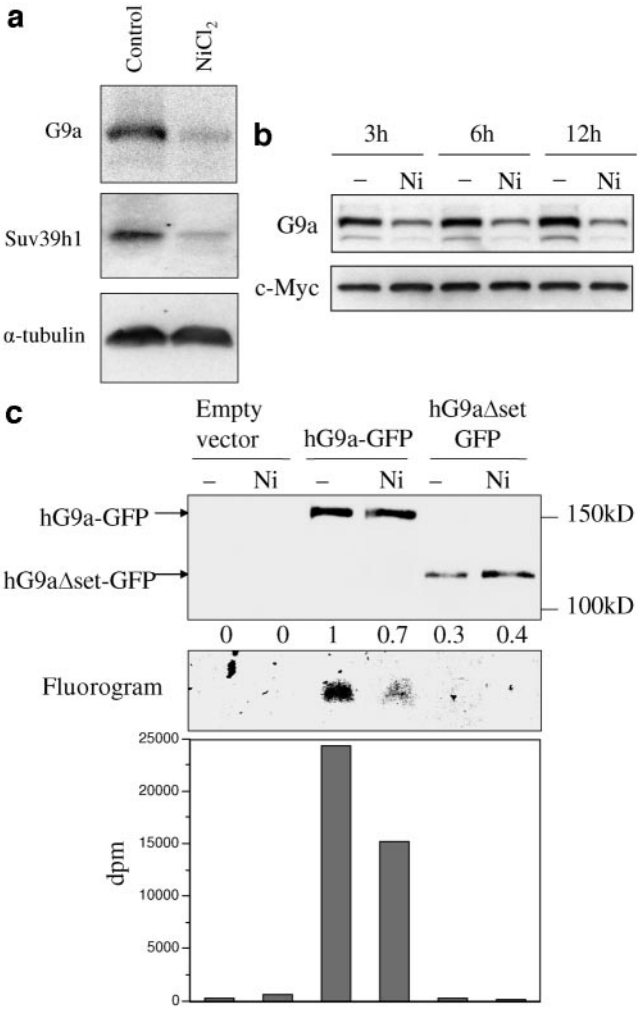

FIG. 2. Nickel ions decreased histone methyltransferase G9a expression and activity. (a) The protein expression of G9a and Suv39h1 in A549 cells following 1 mM $NiCl_2$ exposure for 24 h. After exposure, whole-cell extracts were prepared and analyzed for the expression of G9a and Suv39h1 by immunoblotting. The membranes were restained with α-tubulin antibody to assess the protein loading. (b) A time course study on G9a expression in nuclei of A549 cells following nickel ion exposure. A549 cells were exposed to 1 mM $NiCl_2$, and the nuclear extracts were prepared at the indicated time intervals. Equal amounts of nuclear extracts were separated in an SDS-polyacrylamide gel and analyzed for the expression of G9a using immunoblotting. The membranes were restained with c-Myc antibody to assess the protein loading. (c) Nickel ions decreased G9a methyltransferase activity. HEK 293 cells were transiently transfected with EGFP, EGFP-hG9a, or EGFP-hG9a ΔSET expression vectors and then exposed to 1 mM $NiCl_2$ for 24 h. The cells were lysed in ice-cold RIPA buffer. The expression of fusion proteins in whole-cell lysates was analyzed by immunoblotting with anti-GFP antibody. The methyltransferase activity of overexpressed proteins was measured as described in Materials and Methods.

synthesis was prevented, this decrease of histone labeling represented the removal of histone methylation modifications. Without increasing toxicity in cells, the presence of nickel ions had more ^3H labeling retained on histones following an additional 48-h chase (Fig. 3b). These results suggested that the removal of histone methylation was hindered by Ni ions. Collectively, these results suggested that Ni ions increase H3K9 dimethylation by interfering with the demethylation process.

Nickel ions inhibited a putative Fe(II)–2-oxoglutarate-dependent histone H3K9 demethylase. Histone H3K9 methylation had long been thought of as a permanent modification, and the methylation removal process was poorly understood. Trewick et al. proposed that histone methylation could be removed by oxidation of the methyl group, and this process is likely to be catalyzed by a Fe(II)–2-oxoglutarate-dependent dioxygenase(s) (38). The recent discovery of JHDM1 is the first supportive evidence for the existence of such a histone demethylase. To examine whether such a proposed oxidative demethylation mechanism could be responsible for the removal of H3K9 dimethylation, A549 cells were exposed to several chemicals/conditions that are likely to inhibit the activity of this proposed enzyme. As shown in Fig. 4a, low oxygen (hypoxia), 2-oxoglutarate analog (DMOG), and iron depletion (deferoxamine [DFX]) all substantially increased global H3K9 dimethylation in A549 cells, suggesting that the removal of H3K9 dimethylation may be catalyzed by an iron- and 2-oxoglutarate-dependent demethylase.

To further investigate the nature of this demethylation process, a histone H3K9 demethylation reaction was set up to monitor the removal of ^3H-labeled histone H3K9 methylation in vitro. As shown in Fig. 4b, the removal of histone H3K9 methylation was catalyzed by an enzyme(s), since there was no loss of ^3H radioactivity with the heated nuclear extract. The demethylation process was attenuated in the absence of Fe or 2-oxoglutarate and completely blocked by the addition of DFX (Fig. 4b), indicating a requirement for both iron and 2-oxoglutarate as cofactors. In agreement with the aforementioned results, the presence of Ni ions significantly decreased this demethylation activity. Although the enzyme(s) responsible for this H3K9 demethylation activity remains unidentified, these results strongly suggest the existence of a Fe(II)–2-oxoglutarate-dependent histone H3K9 demethylase(s), whose inhibition by Ni ions likely caused the increase of histone H3K9 dimethylation.

Nickel ions silenced the expression of the *gpt* transgene via epigenetic mechanisms. To investigate whether nickel ion-induced H3K9 dimethylation may lead to gene silencing, the G12 cell system was utilized. We first studied whether nickel ion exposure suppressed the expression of the *gpt* transgene. As shown in Fig. 5a and b, both acute and chronic exposure to nickel ions decreased the expression of the *gpt* transgene in G12 cells.

To examine whether the suppression of the *gpt* transgene by nickel ions can lead to its long-term silencing, G12 cells were exposed to nickel ions for up to 25 days and then selected for the gpt^- phenotype by growing the cells in the presence of 6-TG. It was found that nickel ion exposure increased frequencies of 6-TG^r variants in a dose- and time-dependent manner (Fig. 6a). Since other mechanisms (e.g., mutations or deletions in the *gpt* locus) may also generate the gpt^- phenotype in G12 cells, Ni(II)-induced 6-TG^r variants were treated with 5-Aza. As shown in Fig. 6b, 5-Aza treatment resulted in a very high percentage of reversion from gpt^- to gpt^+ phenotype in the mass population of Ni(II)-induced 6-TG^r variants, while only a few colonies survived HAT selection in the same mass population without 5-Aza treatment. Since reversions to gpt^+ phe-

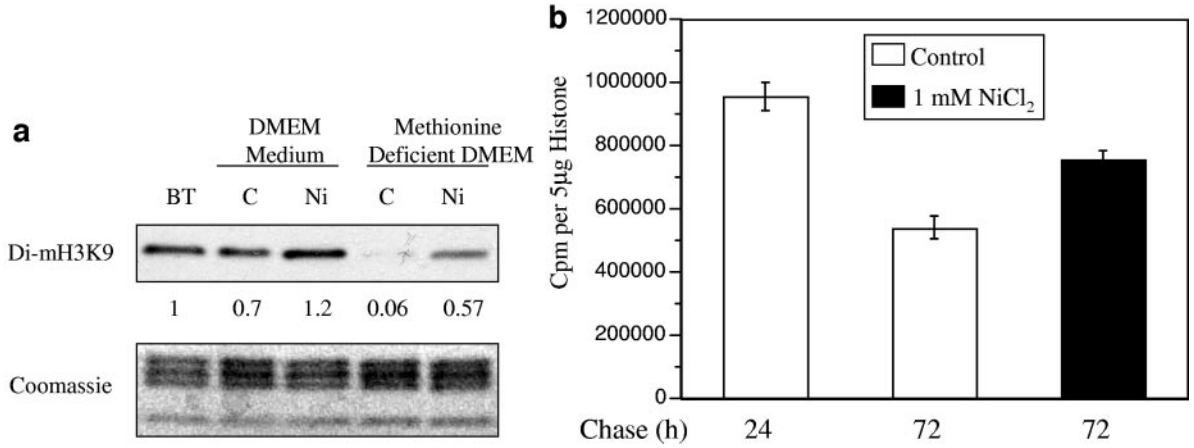

FIG. 3. Nickel ions increased H3K9 dimethylation by inhibiting the histone demethylation process. (a) A549 cells were seeded with F-12–K complete medium. On the second day, cells were replenished with complete DMEM or methionine-deficient DMEM. After incubation for 4 h, cells were then exposed to 1 mM $NiCl_2$ for 24 h. Histones were extracted and immunoblotted for dimethyl-H3K9. BT represents the histones extracted from A549 cells in DMEM before the administration of $NiCl_2$ treatment. (b) Nickel ions decreased the removal rate of histone methylation. A549 cells were radiolabeled with L-[methyl-^{3}H]methionine in methionine-deficient DMEM for 24 h and then replenished with F-12–K complete medium supplemented with 1 mM hydroxyurea. After incubation for 24 h, cells were exposed to 1 mM $NiCl_2$ for an additional 48 h in the presence of hydroxyurea. Histones were extracted, and the radioactivity was measured with a scintillation counter. The experiment was conducted in triplicate.

notype would not be possible in 6-TG^r variants possessing either a deletion or a mutation in the *gpt* locus (22), such a high frequency of reversion to *gpt*$^+$ phenotype indicated that the Ni ion silenced the *gpt* transgene through an epigenetic mechanism.

Role of histone H3K9 dimethylation in the *gpt* transgene silencing by nickel ions. To study the role of histone H3K9 dimethylation in the Ni(II)-induced *gpt* transgene silencing, we first examined the change of global dimethylation in G12 cells following exposure to nickel ions. As shown in Fig. 7a, 100μM nickel ions induced a higher level of H3K9 dimethylation than the 50 μM concentration during the first 3 days of exposure, but similar increases were induced by both concentrations of nickel ions at later time intervals.

To investigate whether the Ni(II)-induced H3K9 dimethylation occurred at the promoter region of the *gpt* transgene, the ChIP assay was utilized. Although an increase of H3K9 dimethylation was found to associate with the *gpt* promoter in the Ni(II)-treated 6-TG^r variants, such an increase was not observed in the Ni(II)-treated cells without 6-TG selection (Fig. 7b). This result is likely due to the heterogeneous nature of the *gpt* transgene expression in Ni(II)-exposed cells without 6-TG selection. By increasing the amount of chromatin input in the ChIP assay, an increase of H3K9 dimethylation at the *gpt*

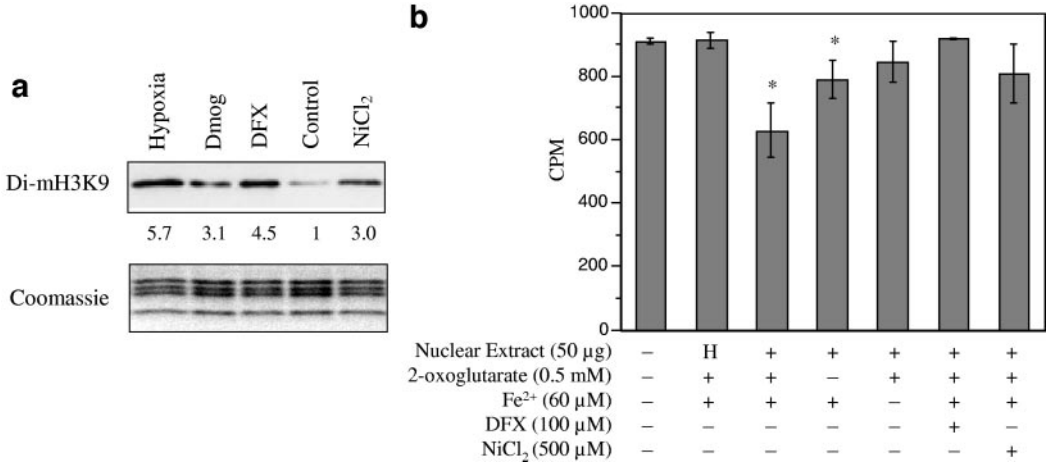

FIG. 4. Nickel ions inhibited the activity of a putative histone H3K9 demethylase. (a) A549 cells were exposed to hypoxia (0.5% O_2 and 99.5% N_2), 1 mM DMOG, 100 μM DFX, or 1 mM $NiCl_2$ for 24 h. Histones were extracted and subjected to dimethyl-H3K9 immunoblotting. (b) Nickel ions inhibited the activity of a putative Fe(II)- and 2-oxoglutarate-dependent histone H3K9 demethylation in vitro. The histone H3K9 demethylation assay was performed as described in Materials and Methods. Each condition was used in duplicate. Two independent experiments were performed, and one representative set of results is shown here. The asterisks represent the statistically significant decrease ($P < 0.05$) compared with the readings in samples with the addition of boiled nuclear extract (H).

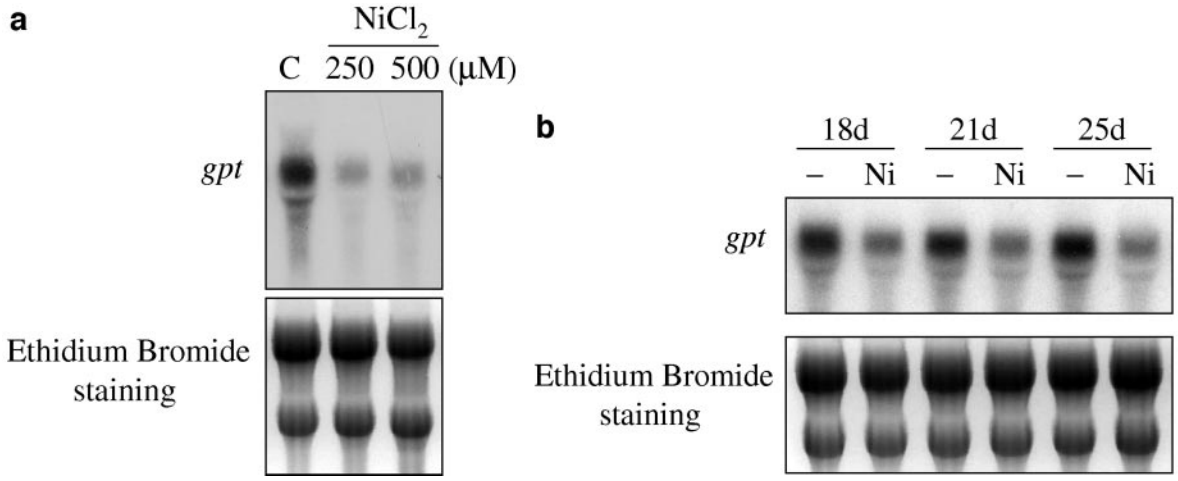

FIG. 5. Nickel ions suppressed the expression of the *gpt* transgene in G12 cells. (a) G12 cells were exposed to various concentrations of $NiCl_2$ for 24 h. (b) G12 cells were exposed to 100 μM $NiCl_2$ for selected time intervals. Total RNA was isolated, and the expression of the *gpt* transgene was examined using Northern blotting. The ethidium bromide staining of total RNA was performed to assess the RNA loading.

promoter was detected in Ni(II)-exposed cells without 6-TG selection (Fig. 7b). In agreement with previous reports that a loss of H3K4 dimethylation is associated with gene repression (19, 28), there was less H3K4 dimethylation at the *gpt* promoter in both Ni(II)-exposed cells and their 6-TG^r variants (Fig. 7b). These results indicated that the increase of H3K9 dimethylation likely played an important role in epigenetic silencing of the *gpt* transgene following Ni ion exposure.

DISCUSSION

Nickel compounds are potent human and animal carcinogens (17), and occupational exposure to these compounds increases the risk of lung and nasal cancers (31). Our previous studies have demonstrated that insoluble nickel compounds silenced transgene expression via epigenetic mechanisms (22, 34). How such epigenetic silencing occurs, however, is not well

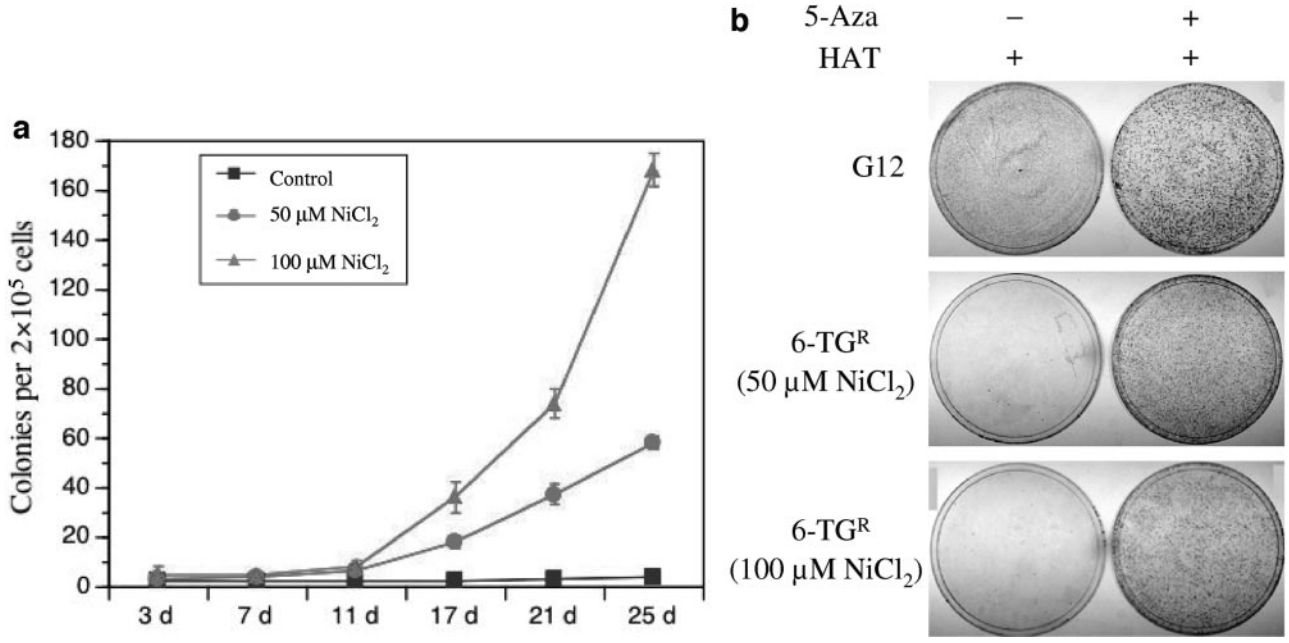

FIG. 6. Nickel ions silenced the *gpt* transgene via epigenetic mechanisms. (a) G12 cells were exposed to various concentrations of $NiCl_2$ for selected time intervals. After a 7-day recovery period, the cells were selected in a medium containing 6-TG (10 μg/ml) for the variants with *gpt*$^-$ phenotype. The data represent the values of observable colonies normalized by cell survival rates. (b) The mass population of Ni(II)-induced 6-TG^r G12 variants as well as G12 cells was treated with or without 4 μM 5-aza-2′-deoxycytidine for 2 days. After a 7-day recovery period, the cells were selected in HAT medium for *gpt*$^+$ phenotype. The surviving colonies were stained with Giemsa stain.

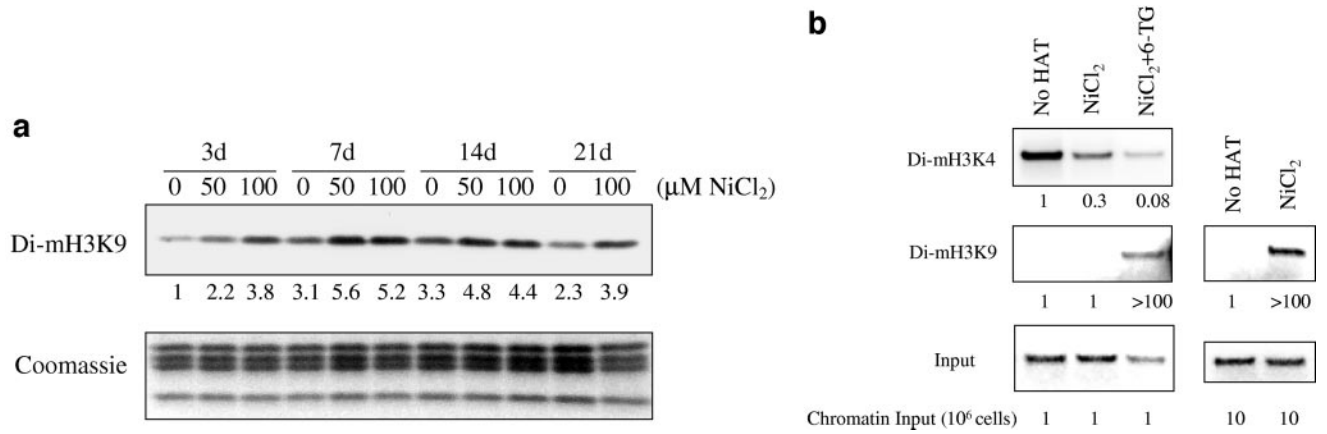

FIG. 7. Association of H3K9 dimethylation with the *gpt* locus following nickel ion exposure. (a) The changes in global H3K9 dimethylation in G12 cells during the course of an extended Ni(II) exposure. G12 cells were exposed to either 50 or 100 μM $NiCl_2$ for selected time intervals. The histones were extracted and immunoblotted for dimethyl-H3K9. (b) Ni(II) exposure increased the occurrence of H3K9 dimethylation at the promoter of the *gpt* transgene. The chromatin from either 1×10^6 or 1×10^7 cells as indicated was subjected to ChIP assays. Input DNA fractions were amplified by PCR to assess the chromatin loading. A set of representative results is shown from two independent experiments. No HAT, G12 cells without HAT selection for 28 days; $NiCl_2$, G12 cells exposed to 100 μM $NiCl_2$ for 28 days; $NiCl_2$ + 6-TG, G12 cells exposed to 100 μM $NiCl_2$ for 28 days and then selected with 6-TG for 10 days.

understood. In this study, we investigated the effects of nickel ion exposure on histone H3K9 dimethylation. Our data strongly indicate that the increase of H3K9 dimethylation plays a pivotal role in Ni(II)-induced *gpt* transgene silencing in G12 cells. Importantly, our results demonstrated the existence of an as-yet-unidentified Fe(II)–2-oxoglutarate-dependent H3K9 demethylase, whose inactivation during nickel ion exposure likely caused the increase of global H3K9 dimethylation.

In the process of identifying the cause of Ni(II)-induced H3K9 dimethylation, the role of H3K9 specific methyltransferase G9a was first examined. It has been reported that G9a plays a dominant role in euchromatic H3K9 dimethylation, and knocking out G9a resulted in a striking loss of global H3K9 dimethylation in mouse cells (35). G9a-mediated H3K9 methylation has also been implicated in gene silencing by interacting with several transcriptional factors, including NRSF/REST, CDP/*cut*, PRDI-BF1/Blimp-1, and SHP (2, 16, 25, 30). However, nickel ion exposure was found to decrease both the expression and activity of G9a. In addition, the expression of another H3K9 methyltransferase, Suv39h1, was also decreased following nickel ion exposure. Our data demonstrated that nickel ions increased H3K9 dimethylation by inhibiting the demethylation process, as was evident from the finding that nickel ions increased H3K9 dimethylation even when the intracellular methylation process was inhibited by the withdrawal of methionine from the medium.

Recently, histone H3K4 demethylase LSD1 has been reported to demethylate H3K9 dimethylation when associated with androgen receptor in human LNCaP prostate tumor cells (24). However, this process should not represent a universal mechanism to demethylate H3K9 because the androgen receptor gene is not expressed in many cells such as the lung carcinoma A549 cells utilized in this study. In addition, deprenyl hydrochloride, a monoamine oxidase inhibitor reported to abolish LSD1 activity (24), failed to increase H3K9 dimethylation in A549 cells (data not shown). Thus, the H3K9 demethylation in A549 cells is likely catalyzed by a demethylase(s) using a mechanism that differs from the amine oxidation caused by LSD1. Further investigation demonstrated that the H3K9 demethylation process could be catalyzed by an as-yet-unidentified 2-oxoglutarate–Fe(II)-dependent dioxygenase(s), and the inhibition of such an H3K9 demethylase(s) by nickel ions was likely responsible for the observed Ni(II)-induced H3K9 dimethylation. To our knowledge, we are the first to detect a histone H3K9 demethylase activity dependent on both iron and 2-oxoglutarate in vitro. It was noticed that a small decrease of H3K9 methylation was still present without the addition of exogenous Fe(II) or 2-oxoglurate. These observations were likely due to the presence of cell-derived iron and 2-oxoglutarate in nuclear extract, since the demethylation activity was completely blocked by addition of an iron chelator, deferoxamine. In fact, it is not surprising that such an H3K9 demethylase exists, because the oxidative demethylation mechanism proposed by Trewick et al. is theoretically plausible (38) and recently validated by the discovery of H3K36 demethylase JHDM1 (39).

Both mono- and dimethylated H3K9s are likely to be the substrates of this unidentified H3K9 demethylase, because these two types of modifications were predominant in the G9a-methylated H3K9 peptide that was added into the in vitro demethylation assay. Although it has been reported that G9a can trimethylate H3K9 in vitro (8, 26), it was unlikely to generate trimethylated H3K9 under the conditions used in our study. In order to generate trimethylated H3K9 in vitro, an excessive amount of SAM in proportion to the substrate was required. For instance, a 25 molar ratio of SAM to H3K9 peptide (250 μM SAM/10 μM peptide) was used in the study by Collins et al. (8), and a 5.2 molar ratio (1 mM SAM/192 μM peptide) was used in another study (26). Here, a 0.27 molar ratio of SAM to H3K9 peptide (1.61 μM SAM/6 μM peptide) was utilized. Considering that addition of a methyl group to an unmethylated peptide was sevenfold faster than that to a dimethylated H3K9 peptide (26), the presence of excessive unmethylated peptide would effectively prevent the generation of

trimethylated H3K9. Therefore, the final labeled mH3K9 peptide following an overnight incubation with G9a was most likely to be mono- and dimethylated H3K9 peptides. This notion is in agreement with the findings that nickel ion exposure increased both mono- and dimethylated H3K9 but not trimethylated H3K9 in A549 cells. Interestingly, JHDM1 has been reported to demethylate H3K36 mono- and dimethylation but not trimethylation (39). Thus, there is still no evidence for the existence of lysine trimethylation demethylase.

The inhibition of H3K9 demethylase by nickel ion was likely due to its interference with function of the iron moiety in this unidentified enzyme(s). Recently, we demonstrated that nickel ions perturbed cellular iron homeostasis (6) and inhibited the enzymes with an [Fe-S] cluster in the cellular energy metabolism pathway (5). In addition, nickel compounds are known to inhibit dioxygenases (prolyl hydroxylase PHD2) responsible for HIF-1α hydroxylation by interfering with the Fe moiety in this enzyme (11, 12). Since a similar mechanism (2-His-1-carboxylate triad motif in sequence) is utilized to bind iron in the Fe(II)–2-oxoglutarate dioxygenase family (4), it is logical to assume that the presence of nickel ions may also interfere with the binding and/or function of Fe(II) in this unidentified H3K9 demethylase. However, the possibility that nickel ion indirectly inhibits this unidentified H3K9 demethylase(s) cannot be excluded at this time. The exact inhibitory mechanism still awaits the identification and purification of this H3K9 demethylase(s).

The Ni(II)-induced H3K9 dimethylation likely initiated the long-term *gpt* transgene silencing in G12 cells. The H3K9 dimethylation identified at the *gpt* promoter region was likely catalyzed by G9a, although nickel ions were shown to decrease G9a protein level and activity in A549 cells. In fact, the inhibition of the H3K9 demethylation process was more prominent than that of the H3K9 methylation process since the global H3K9 dimethylation increased following Ni exposure. Because H3K9 dimethylation is a critical mark for DNA methylation and long-term gene silencing (18), a persistent increase of H3K9 dimethylation during the extended nickel ion exposure may eventually lead to the establishment of DNA methylation at the *gpt* promoter region and the silencing of this transgene. This notion is in agreement with the observations that there was a time lag between the elevation of global H3K9 dimethylation and the increase in the frequency of the gpt^- phenotype following nickel ion exposure, as well as the observation that the gpt^- phenotype was readily reversed by 5-aza-2′-deoxycytidine treatment. Additional histone modifications were altered following nickel ion exposure, such as a striking decrease of both histone acetylation (15, 20) and H3K4 dimethylation (Fig. 7b), which may act in concert to repress the expression of the *gpt* transgene. In agreement, a recent study of an endogenous gene silencing process reported that both H3 deacetylation and H3K9 methylation occurred within the same time frame as gene inactivation, and these changes preceded the establishment of a long-term mark of gene silencing (DNA methylation) at the promoter region of this gene (33).

Although water-soluble nickel salts were shown to increase H3K9 dimethylation and silence the *gpt* transgene in this study, it should be noted that human exposure to water-soluble nickel compounds generally occurs at lower concentrations than has been utilized here. This is because in vivo nickel ions are constantly washed out from the body through excretion (17). The rapid clearance of nickel ions in vivo may explain the lowered incidence of cancer for soluble nickel compounds in animal models (17). Nevertheless, these data are in support of the carcinogenicity of water-insoluble nickel compounds. Because water-insoluble nickel compounds are phagocytosed by the cells, they dissolve in the endosome and release high concentrations of nickel ions into both the cytoplasm and the nucleus (9, 10). This notion is supported by the fact that a similar frequency (10^{-3}) of 6-TG^r variants was achieved by chronic nickel ion exposure and by a 24-h treatment with crystalline nickel subsulfide (Ni_3S_2) (22). Therefore, these results provide an argument that nickel ions released from insoluble nickel compounds are active in the induction of gene silencing.

In conclusion, the results reported here indicated that nickel ions induce transgene silencing by increasing histone H3K9 dimethylation. This Ni(II)-induced H3K9 dimethylation is caused by the inhibition of a histone demethylation enzyme(s) that is likely similar to the prolyl-hydroxylases in their requirement for Fe(II) and 2-oxoglutarate. Future work should be directed at identifying these proposed enzymes. Although the exact histone demethylase targeted by nickel ions is still unidentified, the increase of global H3K9 methylation and subsequent gene silencing by nickel ions is likely to be a key event in nickel carcinogenesis.

ACKNOWLEDGMENTS

We thank Juliana Powell for her excellent secretarial support and also thank Martin Walsh for providing pEGFP-G9a and pEGFP-G9a(ΔSET) expression vectors.

This work was supported by grants ES00260, ES10344, and T32-ES07324 from the National Institute of Environmental Health Sciences and CA16087 from the National Cancer Institute.

REFERENCES

1. **Balciunas, D., and H. Ronne.** 2000. Evidence of domain swapping within the jumonji family of transcription factors. Trends Biochem. Sci. **25:**274–276.
2. **Boulias, K., and I. Talianidis.** 2004. Functional role of G9a-induced histone methylation in small heterodimer partner-mediated transcriptional repression. Nucleic Acids Res. **32:**6096–6103.
3. **Broday, L., W. Peng, M. H. Kuo, K. Salnikow, M. Zoroddu, and M. Costa.** 2000. Nickel compounds are novel inhibitors of histone H4 acetylation. Cancer Res. **60:**238–241.
4. **Bruick, R. K.** 2003. Oxygen sensing in the hypoxic response pathway: regulation of the hypoxia-inducible transcription factor. Genes Dev. **17:**2614–2623.
5. **Chen, H., and M. Costa.** Effects of soluble nickel on cellular energy metabolism in A549 cells. Exp. Biol. Med., in press.
6. **Chen, H., T. Davidson, S. Singleton, M. D. Garrick, and M. Costa.** 2005. Nickel decreases cellular iron level and converts cytosolic aconitase to iron-regulatory protein 1 in A549 cells. Toxicol. Appl. Pharmacol. **206:**275–287.
7. **Clissold, P. M., and C. P. Ponting.** 2001. JmjC: cupin metalloenzyme-like domains in jumonji, hairless and phospholipase A2beta. Trends Biochem. Sci. **26:**7–9.
8. **Collins, R. E., M. Tachibana, H. Tamaru, K. M. Smith, D. Jia, X. Zhang, E. U. Selker, Y. Shinkai, and X. Cheng.** 2005. In vitro and in vivo analyses of a Phe/Tyr switch controlling product specificity of histone lysine methyltransferases. J. Biol. Chem. **280:**5563–5570.
9. **Costa, M., M. P. Abbracchio, and J. Simmons-Hansen.** 1981. Factors influencing the phagocytosis, neoplastic transformation, and cytotoxicity of particulate nickel compounds in tissue culture systems. Toxicol. Appl. Pharmacol. **60:**313–323.
10. **Costa, M., J. Simmons-Hansen, C. W. Bedrossian, J. Bonura, and R. M. Caprioli.** 1981. Phagocytosis, cellular distribution, and carcinogenic activity of particulate nickel compounds in tissue culture. Cancer Res. **41:**2868–2876.
11. **Davidson, T., H. Chen, M. D. Garrick, G. D'Angelo, and M. Costa.** 2005. Soluble nickel interferes with cellular iron homeostasis. Mol. Cell. Biochem. **279:**157–162.
12. **Davidson, T. L., H. Chen, D. M. D. Toro, G. D'Angelo, and M. Costa.** Soluble nickel inhibits HIF-prolyl-hydroxylases creating persistent hypoxic signaling in A549 cells. Mol. Carcinog., in press.

13. **Falnes, P. O.** 2004. Repair of 3-methylthymine and 1-methylguanine lesions by bacterial and human AlkB proteins. Nucleic Acids Res. **32:**6260–6267.
14. **Farooqui, J. Z., H. W. Lee, S. Kim, and W. K. Paik.** 1983. Studies on compartmentation of S-adenosyl-L-methionine in Saccharomyces cerevisiae and isolated rat hepatocytes. Biochim. Biophys. Acta **757:**342–351.
15. **Golebiowski, F., and K. S. Kasprzak.** 2005. Inhibition of core histones acetylation by carcinogenic nickel(II). Mol. Cell. Biochem. **279:**133–139.
16. **Gyory, I., J. Wu, G. Fejer, E. Seto, and K. L. Wright.** 2004. PRDI-BF1 recruits the histone H3 methyltransferase G9a in transcriptional silencing. Nat. Immunol. **5:**299–308.
17. **International Agency for Research on Cancer.** 1990. Chromium, nickel and welding. IARC Monogr. Eval. Carcinog. Risks Hum. **49:**1–648.
18. **Jackson, J. P., L. Johnson, Z. Jasencakova, X. Zhang, L. PerezBurgos, P. B. Singh, X. Cheng, I. Schubert, T. Jenuwein, and S. E. Jacobsen.** 2004. Dimethylation of histone H3 lysine 9 is a critical mark for DNA methylation and gene silencing in Arabidopsis thaliana. Chromosoma **112:**308–315.
19. **Jenuwein, T., and C. D. Allis.** 2001. Translating the histone code. Science **293:**1074–1080.
20. **Kang, J., Y. Zhang, J. Chen, H. Chen, C. Lin, Q. Wang, and Y. Ou.** 2003. Nickel-induced histone hypoacetylation: the role of reactive oxygen species. Toxicol. Sci. **74:**279–286.
21. **Klein, C. B., and M. Costa.** 1997. DNA methylation, heterochromatin and epigenetic carcinogens. Mutat. Res. **386:**163–180.
22. **Lee, Y. W., C. B. Klein, B. Kargacin, K. Salnikow, J. Kitahara, K. Dowjat, A. Zhitkovich, N. T. Christie, and M. Costa.** 1995. Carcinogenic nickel silences gene expression by chromatin condensation and DNA methylation: a new model for epigenetic carcinogens. Mol. Cell. Biol. **15:**2547–2557.
23. **Matranga, C. B., and G. I. Shapiro.** 2002. Selective sensitization of transformed cells to flavopiridol-induced apoptosis following recruitment to S-phase. Cancer Res. **62:**1707–1717.
24. **Metzger, E., M. Wissmann, N. Yin, J. M. Muller, R. Schneider, A. H. Peters, T. Gunther, R. Buettner, and R. Schule.** 2005. LSD1 demethylates repressive histone marks to promote androgen-receptor-dependent transcription. Nature **437:**436–439.
25. **Nishio, H., and M. J. Walsh.** 2004. CCAAT displacement protein/cut homolog recruits G9a histone lysine methyltransferase to repress transcription. Proc. Natl. Acad. Sci. USA **101:**11257–11262.
26. **Patnaik, D., H. G. Chin, P. O. Esteve, J. Benner, S. E. Jacobsen, and S. Pradhan.** 2004. Substrate specificity and kinetic mechanism of mammalian G9a histone H3 methyltransferase. J. Biol. Chem. **279:**53248–53258.
27. **Peters, A. H., D. O'Carroll, H. Scherthan, K. Mechtler, S. Sauer, C. Schofer, K. Weipoltshammer, M. Pagani, M. Lachner, A. Kohlmaier, S. Opravil, M. Doyle, M. Sibilia, and T. Jenuwein.** 2001. Loss of the Suv39h histone methyltransferases impairs mammalian heterochromatin and genome stability. Cell **107:**323–337.
28. **Peterson, C. L., and M. A. Laniel.** 2004. Histones and histone modifications. Curr. Biol. **14:**R546–R551.
29. **Rice, J. C., S. D. Briggs, B. Ueberheide, C. M. Barber, J. Shabanowitz, D. F. Hunt, Y. Shinkai, and C. D. Allis.** 2003. Histone methyltransferases direct different degrees of methylation to define distinct chromatin domains. Mol. Cell **12:**1591–1598.
30. **Roopra, A., R. Qazi, B. Schoenike, T. J. Daley, and J. F. Morrison.** 2004. Localized domains of G9a-mediated histone methylation are required for silencing of neuronal genes. Mol. Cell **14:**727–738.
31. **Shannon, H. S., J. A. Julian, and R. S. Roberts.** 1984. A mortality study of 11,500 nickel workers. J. Natl. Cancer Inst. **73:**1251–1258.
32. **Shi, Y., F. Lan, C. Matson, P. Mulligan, J. R. Whetstine, P. A. Cole, R. A. Casero, and Y. Shi.** 2004. Histone demethylation mediated by the nuclear amine oxidase homolog LSD1. Cell **119:**941–953.
33. **Strunnikova, M., U. Schagdarsurengin, A. Kehlen, J. C. Garbe, M. R. Stampfer, and R. Dammann.** 2005. Chromatin inactivation precedes de novo DNA methylation during the progressive epigenetic silencing of the RASSF1A promoter. Mol. Cell. Biol. **25:**3923–3933.
34. **Sutherland, J. E., W. Peng, Q. Zhang, and M. Costa.** 2001. The histone deacetylase inhibitor trichostatin A reduces nickel-induced gene silencing in yeast and mammalian cells. Mutat. Res. **479:**225–233.
35. **Tachibana, M., K. Sugimoto, M. Nozaki, J. Ueda, T. Ohta, M. Ohki, M. Fukuda, N. Takeda, H. Niida, H. Kato, and Y. Shinkai.** 2002. G9a histone methyltransferase plays a dominant role in euchromatic histone H3 lysine 9 methylation and is essential for early embryogenesis. Genes Dev. **16:**1779–1791.
36. **Tachibana, M., J. Ueda, M. Fukuda, N. Takeda, T. Ohta, H. Iwanari, T. Sakihama, T. Kodama, T. Hamakubo, and Y. Shinkai.** 2005. Histone methyltransferases G9a and GLP form heteromeric complexes and are both crucial for methylation of euchromatin at H3-K9. Genes Dev. **19:**815–826.
37. **Trewick, S. C., T. F. Henshaw, R. P. Hausinger, T. Lindahl, and B. Sedgwick.** 2002. Oxidative demethylation by Escherichia coli AlkB directly reverts DNA base damage. Nature **419:**174–178.
38. **Trewick, S. C., P. J. McLaughlin, and R. C. Allshire.** 2005. Methylation: lost in hydroxylation? EMBO Rep. **6:**315–320.
39. **Tsukada, Y., J. Fang, H. Erdjument-Bromage, M. E. Warren, C. H. Borchers, P. Tempst, and Y. Zhang.** 2006. Histone demethylation by a family of JmjC domain-containing proteins. Nature **439:**811–816.
40. **Yan, Y., T. Kluz, P. Zhang, H. B. Chen, and M. Costa.** 2003. Analysis of specific lysine histone H3 and H4 acetylation and methylation status in clones of cells with a gene silenced by nickel exposure. Toxicol. Appl. Pharmacol. **190:**272–277.